Surface plasmon polariton scattering by finite-size nanoparticles

A. B. Evlyukhin*
Department of Physics and Applied Mathematics, Vladimir State University, Gorkii street 87, Vladimir 600000, Russia

G. Brucoli and L. Martín-Moreno
Departamento de Fisica de la Materia Condensada-ICMA, Universidad de Zaragoza, Zaragoza E-50009, Spain

S. I. Bozhevolnyi
Department of Physics and Nanotechnology, Aalborg University, Skjernvej 4A, DK-9220 Aalborg Ø, Denmark

F. J. García-Vidal
Departamento de Física Teórica de la Materia Condensada, Facultad de Ciencias C-V, Universidad Autónoma de Madrid, E-28049 Madrid, Spain

(Received 24 April 2007; revised manuscript received 13 July 2007; published 20 August 2007)

The electromagnetic Green's tensor approach (GTA) is used to obtain the differential and total scattering cross sections of a finite-size nanoparticle located at a metal surface and illuminated with surface plasmon polaritons (SPPs). The scattering process comprehends either elastic scattering of the incident SPP into other SPPs propagating in different directions or scattering into field components propagating away from the surface, as well as the radiation absorption by the (metal) nanoparticle. Once the total electric field inside the scatterer is known, the expressions obtained allow for a comparison of the efficiency of the different scattering channels. Connection between the GTA and the point-dipole approximation (PDA) of the scattering problem is discussed, including the absorption of the SPP and the transition from the GTA to the PDA when the scatterer is approximated by a spherical particle of the same volume. SPP extinction spectra for gold cubic particles of various sizes placed in the vicinity of a flat gold surface are calculated with the GTA and compared with the results obtained using the PDA.

DOI: 10.1103/PhysRevB.76.075426 PACS number(s): 78.68.+m, 71.36.+c, 02.70.−c, 03.65.Nk

I. INTRODUCTION

Surface plasmon polaritons (SPPs), i.e., surface electromagnetic excitations propagating along metal-dielectric interfaces,[1] are currently attracting a great deal of attention.[2,3] One of the most interesting aspects of SPPs is the possibility of concentrating and guiding electromagnetic radiation at a subwavelength scale by using surface nanostructures. This possibility has been intensively explored in recent experimental and theoretical investigations for a range of nanostructures. SPP wave guiding properties of metallic stripes having widths within the micrometer range have been studied both theoretically[4,5] and experimentally,[6–8] involving SPPs propagation along stripes of finite length and arrangements of narrow slits and indentations.[9–16] Quite recently, the experimental realization of low-loss and well-confined channel plasmon polariton[17] (CPP) propagation along a subwavelength metal groove at telecommunication wavelengths and the realization of different CPP-based subwavelength waveguide components (Y splitter, Mach-Zehnder interferometer, and waveguide-ring resonator) have been reported.[18–20] Another type of SPP-based micro-optical components can be realized by making use of individual metallic nanoparticles arranged to form various structures such as linear chains or two-dimensional arrays. Experimental studies[21–24] showed that nanoparticle ensembles on metal surfaces can be used to create efficient micro-optical components for SPPs, such as mirrors, beam splitters, and interferometers. Furthermore, periodic arrays of metal surface nanoparticles have been shown to exhibit band gap properties for the propagation of SPPs.[25–27] If such a band gap structure has narrow channels free from particles, then SPPs can be confined to and guided along these channels.[27–31]

SPP scattering plays the main role in electromagnetic interactions occurring in ensembles of surface nanoparticles used for the realization of SPP microcomponents. In general, the corresponding scattering problems are very complicated. One of the possible approaches is to make use of the point-dipole approximation[32–34] (PDA) that has successfully been applied to model a number of SPP microcomponents.[35–38] The PDA and its limitations have also been considered in the case of SPP scattering by an individual spherical particle.[34,39]

It is well known that the scattering properties of a particle depend strongly on its shape.[40–43] In order to include in the PDA the influence of the shape of the particle, it was recently suggested to consider a small spheroidal scatterer characterized by its anisotropic free-space polarizability obtained in the long-wavelength (electrostatic) approximation.[38,44] In general, the PDA might fail to properly represent even a very small particle,[45,46] so that one should solve the scattering problem exactly or use other simplifying assumptions. However, the theoretical investigation of SPP scattering processes on various objects is a very intricate problem that requires elaborate numerical calculations even in the relatively simple case of an individual symmetrical scatterer.[47]

In this paper, we present general theoretical considerations of the SPP scattering and attain expressions for the differential and total scattering cross sections for the SPP scattering by a finite-size nanoparticle placed near a planar metal surface. The scattering process includes elastic scatter-

ing of the incident SPP into SPPs propagating in different directions and its (inelastic) scattering into field components propagating away from the surface, as well as radiation absorption by the (metal) nanoparticle. Our calculations are based on the electromagnetic Green's tensor approach (GTA),[48] which is well suited for scattering problems in stratified media.[49–51] We represent the Green's tensor of a metal-dielectric interface system as a sum of several terms each describing the excitation within the system of electromagnetic fields of a certain type: quasistatic or near-field electric field, field of SPPs, and transverse electromagnetic wave propagating away from the metal surface to the far wave zone.[52] Special attention is paid to the connection between the general treatment and the PDA. We calculate the SPP extinction cross sections for a gold nanocube placed near a gold planar surface and analyze the dependence of the extinction spectrum on the size of the cube and on its position with respect to the gold surface. In this case, the dielectric function of the metal in the planar metal-dielectric interface system is assumed to have a negligible imaginary part, while the permittivity of the scatterer has an arbitrary value. Since the PDA is widely exploited for modeling of SPP scattering, we compare the SPP extinction spectra calculated for a finite-size cubic scatterer with those obtained using the PDA. This comparison clarifies a general problem encountered when applying the PDA, which was found to provide only qualitative agreement with experimental results. Throughout this paper, we use the gold permittivity data from Ref. 53 unless otherwise stated.

The paper is organized as follows. Section II presents general considerations of SPP scattering by a finite-size particle. The expressions of the differential and total cross sections for different SPP scattering channels are obtained therein. These results are used to illustrate the connection between the general case based on the GTA and the PDA in Sec. III. In Sec. IV, we present numerical calculations of the SPP extinction spectra for a gold cubic particle placed in the vicinity of a planar gold surface as a function of the system parameters. The exact spectra are then compared with those obtained by using the PDA. The results are summarized, and the conclusions are offered in Sec. V.

II. SURFACE PLASMON POLARITON SCATTERING BY A NANOPARTICLE: GENERAL CONSIDERATION

A. Scattered fields

Let us consider a scattering system (Fig. 1) consisting of a plane electromagnetic surface wave (SPP) that has frequency ω and propagates along the planar interface between two half spaces filled with metal and dielectric with dielectric constants ε_m and ε_r, respectively, such that $-\mathrm{Re}(\varepsilon_m) > \varepsilon_r$. The SPP plane wave is scattered by a macroscopic inhomogeneous object (nanoparticle) localized in the region of volume V and situated at the interface on the dielectric side. In the framework of the Green's function technique, the total electric field in the system is determined by the Lippmann-Schwinger equation[49,54]

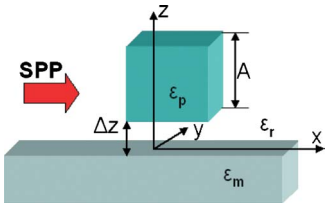

FIG. 1. (Color online) Schematic representation of a scattering system: an SPP monochromatic wave is scattered by a particle with dimension A and dielectric constant ε_p. Δz is the particle-to-surface gap.

$$\mathbf{E}(\mathbf{r}) = \mathbf{E}_0(\mathbf{r}) + k_0^2 \int_V \hat{G}(\mathbf{r},\mathbf{r}')[\varepsilon_p(\mathbf{r}') - \varepsilon_r]\mathbf{E}(\mathbf{r}')d\mathbf{r}', \quad (1)$$

where $\mathbf{E}_0$ is the electric field of the external (incident) SPP wave, k_0 is the wave number in the vacuum, $\hat{G}(\mathbf{r},\mathbf{r}')$ is the Green's tensor of the reference system without the scatterer, ε_p is the dielectric function of the particle, and $\mathbf{E}$ is the total electric field inside the particle. If $\mathbf{r}$ is outside V, then expression (1) describes the superposition between the incident wave and scattered wave (second term on the right-hand side of the equation).

Let us consider (i) an observation point $\mathbf{r}$ located in the far-field zone so that $|\mathbf{r}-\mathbf{r}'| \gg \lambda$ for any $\mathbf{r}'$ inside V (λ is the wavelength of the scattered field) and (ii) that the maximum dimension of the region occupied by the particle L_p is much smaller than the distance between the particle and the observation point as well. Note, however, that the particle may have arbitrary size with respect to the wavelength. The first assumption allows us to use the far-field approximation of the Green's tensor in Eq. (1) and to write the scattered field in the following form:

$$\mathbf{E}_{sc}(\mathbf{r}) = \mathbf{E}_{sc}^{\mathrm{SPP}}(\mathbf{r}) + \mathbf{E}_{sc}^{T}(\mathbf{r}), \quad (2)$$

where $\mathbf{E}_{sc}^{\mathrm{SPP}}$ and $\mathbf{E}_{sc}^{T}$ are the electric fields of the scattered SPPs and the waves propagating away from the metal-dielectric interface, respectively. Here,

$$\mathbf{E}_{sc}^{\mathrm{SPP}(T)}(\mathbf{r}) = k_0^2 \int_V \hat{G}_{\mathrm{SPP}(T)}(\mathbf{r},\mathbf{r}')[\varepsilon_p(\mathbf{r}') - \varepsilon_r]\mathbf{E}(\mathbf{r}')d\mathbf{r}', \quad (3)$$

where $\hat{G}_{\mathrm{SPP}}(\mathbf{r},\mathbf{r}')$ is the far-field approximation of the part of the Green's tensor that governs the excitation of SPPs, and $\hat{G}_T(\mathbf{r},\mathbf{r}')$ is the far-field approximation of the part of the Green's tensor describing s- and p-polarized waves that propagate away from the interface. Here, we have used the fact that, in the case of small absorption of electromagnetic energy in a metal, the Green's tensor of planar metal-dielectric interface system can be represented as a sum of several terms, each describing excitation in the system of electromagnetic fields of a certain type: quasistatic or near-field electric field, field of SPPs, and transverse electromagnetic wave propagating from the metal surface to the far wave zone.[52]

Choosing the origin of a Cartesian coordinate system on the metal-dielectric interface with the z axis directed to the dielectric half space and inside or in close vicinity to the region occupied by the scatterer (see Fig. 1), we can write

$$\hat{G}_{\mathrm{SPP}}(\mathbf{r},\mathbf{r}') = \frac{\tilde{Z}k_P^{1/2}e^{-iZ_sk_P(z+z')}}{(2\pi\rho)^{1/2}}e^{i(k_P[\rho-\mathbf{m}\mathbf{r}_\parallel']-\pi/4)} \times \begin{pmatrix} -Z_s^2\frac{x^2}{\rho^2} & -Z_s^2\frac{xy}{\rho^2} & Z_s\frac{x}{\rho} \\ -Z_s^2\frac{yx}{\rho^2} & -Z_s^2\frac{y^2}{\rho^2} & Z_s\frac{y}{\rho} \\ -Z_s\frac{x}{\rho} & -Z_s\frac{y}{\rho} & 1 \end{pmatrix}, \quad (4)$$

where $Z_s=-i\sqrt{\varepsilon_r/(-\varepsilon_m)}$, $\tilde{Z}=\frac{Z_s}{(1+Z_s^2)(Z_s^4-1)}$, $k_P=k_0\sqrt{\varepsilon_r\varepsilon_m/(\varepsilon_r+\varepsilon_m)}$ is the SPP wave number, $\mathbf{r}=(x,y,z)=(\mathbf{r}_\parallel,z)$ is the radius vector relative to the fields observed in the domain $z\geqslant 0$, $\mathbf{r}'=(x',y',z')=(\mathbf{r}_\parallel',z')$ is the radius vector of a wave source, $\rho=|\mathbf{r}_\parallel|$, and $\mathbf{m}=\mathbf{r}_\parallel/\rho$ is the unit vector directed along $\mathbf{r}_\parallel$. Expression (4) was obtained from the representation of $\hat{G}_{\mathrm{SPP}}$ given in Eq. (25) of Ref. 52. Here, we replaced the Hankel function by its asymptotic expansion at large distances and used the approximation $|\mathbf{r}_\parallel-\mathbf{r}_\parallel'|\approx\rho-\mathbf{m}\mathbf{r}_\parallel'$.

The tensor $\hat{G}_T(\mathbf{r},\mathbf{r}')$ is the sum of the direct contribution $\hat{G}_0$, which is the Green's tensor of a homogeneous medium with dielectric constant ε_r, and indirect contribution $\hat{G}_S$, which describes reflection from the metal-dielectric interface. Using a general result from Ref. 50, we obtain

$$\hat{G}_0(\mathbf{r},\mathbf{r}') = \frac{e^{ik_rr}}{4\pi r}e^{-ik_r(\mathbf{r}\mathbf{r}')/r}\begin{pmatrix} 1-\frac{x^2}{r^2} & -\frac{xy}{r^2} & -\frac{xz}{r^2} \\ -\frac{yx}{r^2} & 1-\frac{y^2}{r^2} & -\frac{yz}{r^2} \\ -\frac{xz}{r^2} & -\frac{yz}{r^2} & \frac{\rho^2}{r^2} \end{pmatrix} \quad (5)$$

and, representing $\hat{G}_S$ as the sum of the different polarization contributions, p polarization $\hat{G}_S^{p\text{-}pol}$ and s polarization $\hat{G}_S^{s\text{-}pol}$, respectively,

$$\hat{G}_S^{p\text{-}pol}(\mathbf{r},\mathbf{r}') = \frac{e^{ik_rr}}{4\pi r}e^{-ik_r(\mathbf{r}_\parallel\mathbf{r}_\parallel'-zz')/r}r^{(p)} \times \begin{pmatrix} -\frac{x^2z^2}{\rho^2r^2} & -\frac{xyz^2}{\rho^2r^2} & -\frac{xz}{r^2} \\ -\frac{xyz^2}{\rho^2r^2} & -\frac{y^2z^2}{\rho^2r^2} & -\frac{yz}{r^2} \\ \frac{xz}{r^2} & \frac{yz}{r^2} & \frac{\rho^2}{r^2} \end{pmatrix}, \quad (6)$$

$$\hat{G}_S^{s\text{-}pol}(\mathbf{r},\mathbf{r}') = \frac{e^{ik_rr}}{4\pi r}e^{-ik_r(\mathbf{r}_\parallel\mathbf{r}_\parallel'-zz')/r}r^{(s)} \begin{pmatrix} \frac{y^2}{\rho^2} & -\frac{xy}{\rho^2} & 0 \\ -\frac{xy}{\rho^2} & \frac{x^2}{\rho^2} & 0 \\ 0 & 0 & 0 \end{pmatrix}, \quad (7)$$

where $k_r=k_0\sqrt{\varepsilon_r}$, $r=|\mathbf{r}|$, and $r^{(p)}$ and $r^{(s)}$ are the Fresnel reflection coefficients for (p) and (s) polarizations.[34]

Inserting Eq. (4) in Eq. (3), the components of the scattered SPP electric field in the region $z\geqslant 0$ can be written in cylindrical coordinates as

$$E_z^{\mathrm{SPP}}(\mathbf{r}) = \frac{\tilde{Z}k_0^2k_P^{1/2}e^{i(k_P\rho-\pi/4)-iZ_sk_Pz}}{(2\pi\rho)^{1/2}} \times \int_V e^{-ik_P(\mathbf{m}\mathbf{r}_\parallel'+Z_sz')}\Delta\varepsilon(\mathbf{r}')[E_z-Z_s\mathbf{m}\mathbf{E}_\parallel]d\mathbf{r}', \quad (8)$$

where $\Delta\varepsilon(\mathbf{r})=\varepsilon_{\mathbf{p}}(\mathbf{r})-\varepsilon_{\mathbf{r}}$ and $\mathbf{E}_\parallel=(E_x,E_y)$. The other nonzero SPP electric field component is $E_\rho^{\mathrm{SPP}}(\mathbf{r})=Z_sE_z^{\mathrm{SPP}}(\mathbf{r})$. The scattered SPP magnetic field can be found using the Maxwell equations. Thus, we have

$$H_\varphi^{\mathrm{SPP}}(\mathbf{r}) = -\frac{\varepsilon_0^{1/2}}{\mu_0^{1/2}}\frac{k_P}{k_0}(Z_s^{\,2}+1)E_z^{\mathrm{SPP}}(\mathbf{r}), \quad (9)$$

where ε_0 and μ_0 are the vacuum permittivity and permeability, respectively.

Note that the electromagnetic field components in the domain $z<0$ can be obtained from the above expressions applying the boundary conditions under $z=0$ and replacing the factor $\exp(-iZ_sk_Pz)$ by $\exp(-ik_Pz/Z_s)$.

For the electric field of the waves propagating away from the interface, it is convenient to use the spherical coordinates and basis, and inserting Eqs. (5)–(7) in Eq. (3), one gets

$$E_\varphi^T(\mathbf{r}) = \frac{k_0^2e^{ik_rr}}{4\pi r}\int_V e^{-ik_r\mathbf{n}\mathbf{r}'}(1+r^{(s)}e^{ik_r2z'\cos\theta}) \times\Delta\varepsilon(\mathbf{r}')[E_y\cos\varphi-E_x\sin\varphi]d\mathbf{r}', \quad (10)$$

$$E_\theta^T(\mathbf{r}) = \frac{k_0^2e^{ik_rr}}{4\pi r}\int_V e^{-ik_r\mathbf{n}\mathbf{r}'}\Delta\varepsilon(\mathbf{r}')\{(1-r^{(p)}e^{ik_r2z'\cos\theta}) \times(E_x\cos\varphi\cos\theta+E_y\sin\varphi\cos\theta) - E_z\sin\theta(1+r^{(p)}e^{ik_r2z'\cos\theta})\}d\mathbf{r}', \quad (11)$$

where $\mathbf{n}$ is the unit vector directed to the observation point, and φ and θ are the azimuthal and polar angles of the spherical coordinate system, respectively.

B. Scattering cross sections

The efficiency of the different SPP scattering channels is determined by calculating the differential and total cross sections for both scattering channels. Let us assume that the incident field is a plane SPP wave propagating along the interface in the x direction. The normalized electric field $\mathbf{E}_0$

of this SPP can be represented in the following form:[52]

$$\mathbf{E}_0(\mathbf{r}) = \exp(ik_P x - ik_P Z_s z)(Z_s\hat{x}, 0\hat{y}, \hat{z}), \quad z \geqslant 0. \tag{12}$$

The differential cross sections can be determined through the relation between the time-averaged Poynting vectors of incident and scattering waves. Applying the procedure from the previous work,[34] we can consider separately the two SPP scattering channels.

In the case of the SPP-to-SPP scattering, we obtain the differential cross section

$$\sigma_{\mathrm{SPP}}(\varphi) = \frac{-\tilde{Z}^2 k_0^4 k_P}{2\pi} \int_V \int_V e^{-iZ_s k_P(z+z')} e^{-ik_P \mathbf{m}(\mathbf{r}_\parallel - \mathbf{r}'_\parallel)} \Delta\varepsilon(\mathbf{r}) F(\mathbf{r}) \times [\Delta\varepsilon(\mathbf{r}') F(\mathbf{r}')]^* d\mathbf{r} d\mathbf{r}', \tag{13}$$

the sign * denotes the complex conjugation and $F(\mathbf{r}) = E_z(\mathbf{r}) + Z_s[E_x(\mathbf{r})\cos\varphi + E_y(\mathbf{r})\sin\varphi]$. The total cross section for SPP-to-SPP scattering $\sigma_{\text{SPP-SPP}}$ is finally obtained by angular integration of the differential cross section given by Eq. (13):

$$\sigma_{\text{SPP-SPP}} = \int_0^{2\pi} \sigma_{\mathrm{SPP}}(\varphi) d\varphi. \tag{14}$$

For the out-of-plane SPP scattering, the differential cross section can be written down in the spherical coordinates as follows:

$$\sigma_{\text{space}}(\varphi, \theta) = -2ik_r \tilde{Z} |\mathbf{E}_{sc}^T|^2 r^2, \tag{15}$$

and the total cross sections for the two polarizations are given, respectively, by

$$\sigma_{\text{SPP-space}}^{(s(p)\text{-pol})} = \int_0^{2\pi} \int_0^{\pi/2} -2ik_r \tilde{Z} |E_{\varphi(\theta)}^T|^2 r^2 \sin\theta d\varphi d\theta, \tag{16}$$

where the scattered field $\mathbf{E}_{sc}^T$ is given by Eqs. (10) and (11). The total scattering cross section σ_{scat} is the sum of three terms,

$$\sigma_{scat} = \sigma_{\text{SPP-SPP}} + \sigma_{\text{SPP-space}}^{(s\text{-pol})} + \sigma_{\text{SPP-space}}^{(p\text{-pol})}. \tag{17}$$

If scatterer can absorb the electromagnetic energy, then the absorption cross section σ_{abs} is determined by the following expression:

$$\sigma_{abs} = \sigma_{ext} - \sigma_{scat}, \tag{18}$$

where the extinction cross section σ_{ext} can be calculated from the expression[34,55]

$$\sigma_{ext} = \frac{\omega}{2P_{in}} \mathrm{Im} \int_V \mathbf{E}_0^*(\mathbf{r}') \varepsilon_0 \Delta\varepsilon(\mathbf{r}') \mathbf{E}(\mathbf{r}') d\mathbf{r}', \tag{19}$$

where

$$P_{in} = \frac{1}{2k_0} \sqrt{\frac{\varepsilon_0}{\mu_0}} \frac{i}{2\tilde{Z}} \tag{20}$$

is the incident SPP power per unit length with the electric field [Eq. (12)].[34] Finally, we obtain

$$\sigma_{ext} = -2ik_0^2 \tilde{Z}\, \mathrm{Im} \int_V \mathbf{E}_0^*(\mathbf{r}')[\varepsilon_p(\mathbf{r}') - \varepsilon_r] \mathbf{E}(\mathbf{r}') d\mathbf{r}'. \tag{21}$$

Note that due to the two-dimensional character of SPPs, $\sigma_{ext} \sim k_0^2$ and has dimension [length] [recall that the fields in Eq. (21) are normalized as in Eq. (12)], whereas for the scattering of light in uniform space, $\sigma_{ext} \sim k_0$ with dimension [length^2]; as a result, the SPP extinction cross section decreases faster than free-propagating light with an increasing wavelength.

If the absorption energy in the scatterer is equal to zero, then $\sigma_{ext} = \sigma_{scat}$, and we have two relatively independent methods for calculating the total scattering cross section. This gives us a way of testing the numerical modeling of SPP scattering phenomena.

III. POINT-DIPOLE APPROXIMATION

If the largest dimension L_p of a scattering particle is smaller than $1/k_P$ (as a consequence smaller than $1/k_r$), then expanding the total scattering cross section with respect to the $k_P L_p$ ($k_r L_p$), we can represent the cross section as the sum of multipole cross sections $\sigma_{scat}^{(i)}$:

$$\sigma_{scat} = \sigma_{scat}^{(0)} + \sigma_{scat}^{(1)} + \sigma_{scat}^{(2)} + \cdots. \tag{22}$$

For example, the differential SPP-to-SPP scattering cross section in the PDA can be written as the follows:

$$\sigma_{\mathrm{SPP}}^{(0)}(\varphi) = \frac{-\tilde{Z}^2 k_0^4 k_P V^2}{2\pi} |\langle \Delta\varepsilon F(\varphi) \rangle|^2 e^{-2iZ_s k_P z_p}, \tag{23}$$

where z_p is the position of the scatterer center along the z direction, $\langle \Delta\varepsilon F(\varphi) \rangle = \langle \Delta\varepsilon E_z \rangle - Z_s[\langle \Delta\varepsilon E_x \rangle \cos\varphi + \langle \Delta\varepsilon E_y \rangle \sin\varphi]$,

$$\langle \Delta\varepsilon \mathbf{E} \rangle = \int_V \Delta\varepsilon \mathbf{E}(\mathbf{r}) d\mathbf{r}/V. \tag{24}$$

Thus, in the PDA, the scattering cross sections and the scattered fields are determined by the average total electric field with the weight $\Delta\varepsilon = (\varepsilon_p - \varepsilon_r)$ in the scatterer.

Note that the combination $\varepsilon_0 V \langle \Delta\varepsilon \mathbf{E} \rangle$ is the dipole moment $\mathbf{p} = (p_x, p_y, p_z)$ of the scatterer.

The total electric field inside the region occupied by a scatterer can be obtained from Eq. (1). In general, the solutions must be computed numerically, even in the near-field (quasistatic) approach, using the GTA. In this approach, the scatterer is discretized into a number of sampling volumes inside of which the electric field, taken to be constant, is determined by solving a set of linear simultaneous equations for the field at every sample point.[49] Thus, after the discretizing procedure, the integrals in Eq. (1) and in the expressions of the differential scattering cross sections are replaced by integral sums.

However, there is a case in which the electric field inside a scatterer can be obtained analytically from Eq. (1) with very good accuracy. This is the case of the scattering of a SPP plane waves by an individual small uniform spherical particle. If the position, size, and dielectric constant of the

particle satisfy certain conditions, the total electric field inside the particle is independent of the spatial coordinates and is almost uniform. This is a general result of the Rayleigh scattering theory[56] for a small particle near a metal surface. The details of these conditions have been reported elsewhere.[34,39] Particularly in the framework of this approach the SPP wavelength is much larger than the particle's radius and the Green's tensor for the field inside the particle is approximated by the quasistatic part only. Furthermore, the gap between the particle and the metal surface with SPPs should be larger than the particle's size. As a result, the field inside the spherical particle is determined by the following expression:

$$\mathbf{E}(\mathbf{r}_p) = \frac{3\varepsilon_r}{\varepsilon_p + 2\varepsilon_r}\left(\frac{\hat{x}\hat{x}}{1+\xi\beta} + \frac{\hat{y}\hat{y}}{1+\xi\beta} + \frac{\hat{z}\hat{z}}{1+2\xi\beta}\right)\mathbf{E}_0(\mathbf{r}_p), \tag{25}$$

where $\mathbf{r}_p$ is the radius vector to the center point inside the scatterer, and $\hat{x}$, $\hat{y}$, and $\hat{z}$ are the unit vectors of the chosen Cartesian coordinate system. $\beta=[R_p/(2z_p)]^3$ is a geometrical parameter (R_p is the radius of the particle with the volume V_p) and $\xi=[(\varepsilon_r-\varepsilon_m)(\varepsilon_p-\varepsilon_r)]/[(\varepsilon_r+\varepsilon_m)(\varepsilon_p+2\varepsilon_r)]$ a material one. Thus, Eq. (25) reflects the fact that the role of the surface with SPP can be adjusted equivalently by the system geometry or by the dielectric susceptibilities involved. Introducing the polarizability tensor

$$\hat{\alpha}_d = \frac{3\varepsilon_0\varepsilon_r(\varepsilon_p-\varepsilon_r)V_p}{\varepsilon_p+2\varepsilon_r}\left(\frac{\hat{x}\hat{x}}{1+\xi\beta} + \frac{\hat{y}\hat{y}}{1+\xi\beta} + \frac{\hat{z}\hat{z}}{1+2\xi\beta}\right), \tag{26}$$

we have that the dipole moment of the scatterer is $\mathbf{p}=\hat{\alpha}_d\mathbf{E}_0(\mathbf{r}_p)$. If $\xi\beta \ll 1$, the influence of the surface is negligible and $\mathbf{p}=\hat{\alpha}_0\mathbf{E}_0(\mathbf{r}_p)$ ($\hat{\alpha}_0$ is the quasistatic polarizability tensor of a spherical particle in homogeneous medium). Using the dipole moment of the particle, one obtains the scattered fields and then the scattering cross sections.[34,57] All cross sections are proportional to V_p^2, as in Eq. (23). Note that the total electric field inside SPP scatterer can be almost constant even for a small ellipsoidal particle, if the configuration and material parameters of the system satisfy the same conditions as a small spherical scatterer and if we change the radius of the scatterer by the largest semiaxis of the ellipsoid.[44]

Owing to the relative simplicity of the PDA in the case of a spherical (ellipsoidal) scatterer, this approach is frequently extrapolated on the case of SPP scattering by a particle of arbitrary shape, located just on a metal surface and with a relatively larger size than strictly demanded by the theory. This heuristic approach is widely used for the SPP scattering modeling when one considers nanoparticle surface structures as in various optical microcomponents. Besides qualitative agreements with experimental data,[25,35,37] this approximation allows us to achieve quantitative agreement between modeling and experimental results by including ellipsoidal scatterers in a numerical model.[38] However, one of the main limitations of the point-dipole approximation consists in the impossibility to consider resonance effects appropriately.

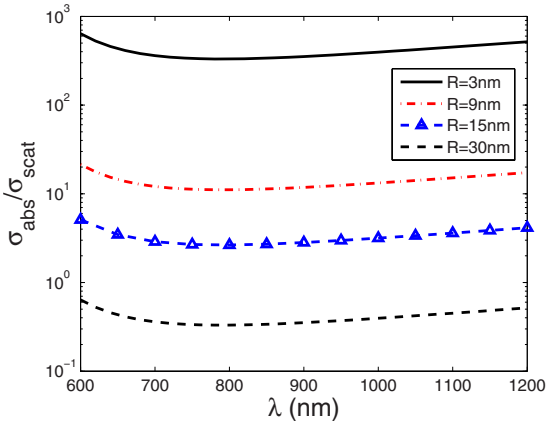

FIG. 2. (Color online) Spectra of $\sigma_{abs}^{\mathrm{PDA}}/\sigma_{scat}^{\mathrm{PDA}}$, calculated in the PDA, for spherical gold scatterers with different radius R located near gold surface. The particle-to-surface gap $\Delta z=50$ nm.

Here, we refer to both configuration resonances[58] and the particle local plasmon resonances. The first is strongly dependent on the particle-to-surface distance and the latter is determined by the particle's shape. Indeed, even in the case of a very small spherical particle in an uniform environment, the dipole approximation is not valid in the region of the shape-dependent localized resonance of the particle if the absorption of electromagnetic energy by the particle is negligible.[45,46] However, if the dielectric constant ε_p has a small, but finite, imaginary part, then the absorption of incident energy can dominate the scattering for a relatively small scatterer. Inserting Eq. (25) into Eq. (21) and using Eq. (12), one can obtain an estimate of the SPP absorption in the framework of the PDA:

$$\sigma_{abs}^{\mathrm{PDA}} = \frac{-\tilde{Z}2ik_0^2 e^{-2iZ_s k_{pz_p}}}{\varepsilon_0}\,\mathrm{Im}\left(\frac{\alpha_0}{1+2\xi\beta}(1+\eta_p)\right), \tag{27}$$

where $\eta_p=-Z_s^2(1+2\xi\beta)/(1+\xi\beta)$. Note that if $\mathrm{Im}(\varepsilon_p)=0$, then σ_{abs} is equal to zero. Taking into account that for a small scatterer located near the surface with SPP the total scattering cross section σ_{scat} has the same order of magnitude as $\sigma_{\mathrm{SPP\text{-}SPP}}$,[34] let us compare σ_{abs} and $\sigma_{\mathrm{SPP\text{-}SPP}}$ in the PDA. The effect of a metal surface on the scatterer's polarizability is small in the PDA; therefore, for the sake of simplicity, we will neglect this influence on the polarizability $\hat{\alpha}_d$ ($\xi\beta \ll 1$) in this approach and for $|\varepsilon_m| \gg 1$ and $|\varepsilon_p| \gg 1$, we obtain

$$\frac{\sigma_{abs}^{\mathrm{PDA}}}{\sigma_{\mathrm{SPP\text{-}SPP}}^{\mathrm{PDA}}} \sim \frac{1}{\pi^3}\frac{\lambda^3}{V}\frac{\mathrm{Im}(\varepsilon_p)}{[\mathrm{Re}(\varepsilon_p)]^2}. \tag{28}$$

Thus, absorption is larger than scattering if the scatterer has a volume

$$V < \frac{\lambda^3}{\pi^3}\frac{\mathrm{Im}(\varepsilon_p)}{[\mathrm{Re}(\varepsilon_p)]^2}. \tag{29}$$

In general, within the PDA, when the spectra of the ratio between $\sigma_{abs}^{\mathrm{PDA}}$ and $\sigma_{scat}^{\mathrm{PDA}}$ are compared for spherical gold scatterers with different radii located near a gold surface (Fig. 2), such ratio is strongly dependent on the size of the

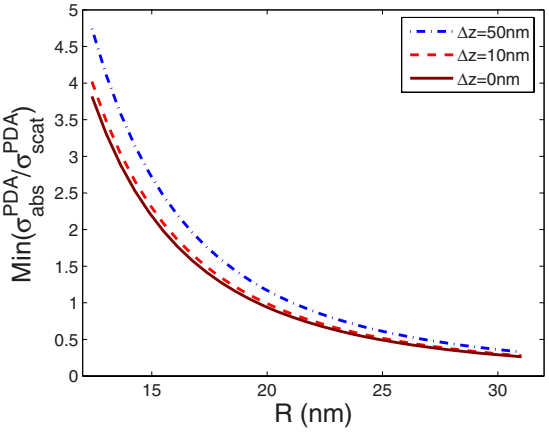

FIG. 3. (Color online) Minimum of $\sigma_{abs}^{\mathrm{PDA}}/\sigma_{scat}^{\mathrm{PDA}}$, calculated in the PDA, as a function of particle's radius R for spherical gold scatterers near gold surface. Δz is the particle-to-surface gap.

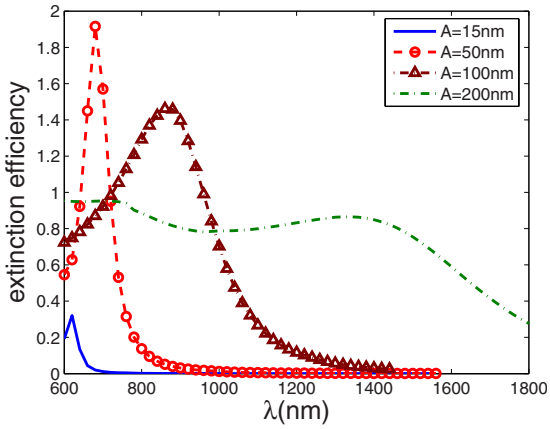

FIG. 4. (Color online) Spectrum of SPP extinction efficiency (σ_{ext}/A), calculated using the GTA, for gold cubic particles with side dimension A. The particle-to-surface gap is $\Delta z=0$.

particle. For scatterers having a radius smaller than 20 nm, absorption is larger than scattering on the whole range of wavelengths (Fig. 3).

In the following section in the framework of the GTA, the SPP extinction cross sections [Eq. (21)] for single gold nanocubes of different sizes placed near a flat gold surface will be calculated in order to study the role of finite-size effects in the SPP scattering problem by a nanoparticle. The results will then be compared with the ones obtained in the framework of the PDA, that is,

$$\sigma_{ext}^{\mathrm{PDA}} = \sigma_{abs}^{\mathrm{PDA}} + \sigma_{scat}^{\mathrm{PDA}}, \tag{30}$$

where $\sigma_{ext}^{\mathrm{PDA}}$ is the extinction cross section calculated with the PDA.

IV. NUMERICAL CONSIDERATION

Let us consider SPP scattering by a single gold particle located near a gold surface. Recently, the electric electromagnetic field distribution of a related system (a noncubic particle placed on a thin metal film, illuminated by a plane wave) has been analyzed.[59,60] Here, we consider on the SPP scattering by a cubic particle with side A, concentrating on the comparison between the GTA and PDA methods. In our study, the particle is separated from the surface by a finite space gap Δz (Fig. 1), defined such that if the particle touches the surface, $\Delta z=0$.

Note that, in the calculation of total electric field inside a scatterer, we use the Green's tensor of a metal-dielectric interface system with no approximation.[52,61] In the numerical procedure, the value of discretization step is determined by the convergence of the solution and depends on the wavelength. When the wavelength is nonresonant (see below), the discretization step has been taken equal to $A/10$; otherwise, it was necessary to take a mesh size equal to $A/20$. The criterion was that a finer discretization step would not practically produce a difference from the value of the cross section obtained in the previous cases.

Let us first consider the case $\Delta z=0$. Figure 4 represents the spectrum of SPP extinction efficiency (σ_{ext}/A) for different sizes of the scattering cube. The resonance peak corresponding to the localized surface plasmon (LSP) mode of the cube appears in the considered wavelength range for relatively small cubes. This mode is excited by the electric field of the incident SPP wave. Detailed discussion of the plasmon eigenmodes for a cubiclike particle in free space can be found in Refs. 42 and 62. Note that the field inside the small cubes (in the quasistatic limit) is determined by the induced electronic charge that is not distributed homogeneously on the surface. As a result, the multipolar charge distributions always exist independently of the cube size. However, the high multipolar LSPs correspond to smaller wavelengths than the dipolar one.[63] When the quasistatic field gives the main contribution in the total field inside the particles (curves for $A=15$ and 50 nm), the resonance extinction efficiency increases as the size of the particle increases, whereas for relatively large particles, this value decreases as the size of the particle increases (Fig. 4). At the same time for the large particles ($A=100$ nm and $A=200$ nm), the peak is broadened because of the contributions of SPPs and of radiation from the total electric field inside the cube. Furthermore, increasing the size of the particle will redshift the resonance wavelength. This behavior is similar to the case of light being scattered by a metal nanoparticle in homogeneous space.[64] However, some features related to the presence of the metal surface can be highlighted. For the small particles ($A=15$ nm and $A=50$ nm), the spectrum difference between the resonance position is equal to approximately 100 nm, whereas for larger particles ($A=100$ nm and $A=200$ nm), this difference is increased to 500 nm (Fig. 4). As a consequence, one may suppose that the redshift, and hence the interaction of a SPP scatterer with a metal surface, is larger for large particles than for small ones. This is confirmed by the results presented in Fig. 5. Comparing the extinction spectra for cubes of the same size located at different distances from the metal surface, two features appear in Fig. 5: First, the red shift of the LSP resonance due to the interaction between the scatterer and the metal surface increases with the size of the cube and, second, the resonance value of extinction cross section is enhanced, especially for the small

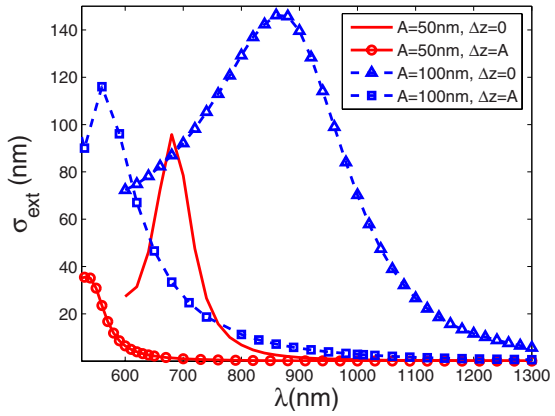

FIG. 5. (Color online) Spectrum of SPP extinction cross section σ_{ext}, calculated using the GTA, for gold cubic particles with side dimension A for different particle-to-surface gaps Δz.

particle when the particle approaches the surface and touches it ($\Delta z=0$). Our calculations have also shown that no significant resonance shift occurs due to the interaction with the surface with SPP when Δz is larger than $A/2$.

Let us now compare the SPP extinction spectra calculated with the GTA for a cubic gold particle placed in the vicinity of a flat gold surface with the results obtained using the PDA when the scatterer is approximated by a spherical particle of the same volume. In the PDA, the spherical particle corresponding to the cube with side dimension A is described by the polarizability tensor $\hat{\alpha}_d$ [Eq. (26)], where the radius $R_p=(3/4\pi)^{1/3}A$ and $z_p=\Delta z+R_p$. For example, for $A=100$ nm and $\Delta z=A$, one obtains $R_p\approx 62.04$ nm and $z_p\approx 162.04$ nm.

The resulting extinction cross sections for 15 and 50 nm cubes are plotted in Figs. 6(a) and 6(b) for $\Delta z=0$ and $\Delta z=A$, respectively. One can see that no resonances appear in the dipole approximation for the considered wavelength range. Moreover, considerable differences exist in all of the represented ranges between the values of the extinction cross sections calculated for finite-size particles and within the framework of the point-dipole approach, for the particles located just on the metal surface [Fig. 6(a)]. Note that the PDA gives a much smaller extinction cross sections than the exact case, not only at resonance but throughout the spectrum. Increasing the distance between the particle and the metal surface hosting SPPs causes the deviation of the PDA results from the finite-size calculations to suddenly decrease [Fig. 6(b)] and become negligible under the condition of a large particle-to-surface distance and nonresonant scattering [$A=50$ nm, Fig. 6(b)]. It is important to stress that the extinction spectra of the cubic particles located close to the surface are practically parallel to the PDA extinctions for the corresponding spherical particles in those regions of the spectrum which are far from resonance [Fig. 6(a), and the curves for $A=15$ nm in Fig. 6(b)]. Only one fitting parameter (the volume or size of scatterer) is sufficient to attain a good agreement between the strict calculation and PDA results for any nonresonant wavelength range (Fig. 6).

The scattering cross section in the point-dipole approximation is proportional to V^2; therefore, its value increases

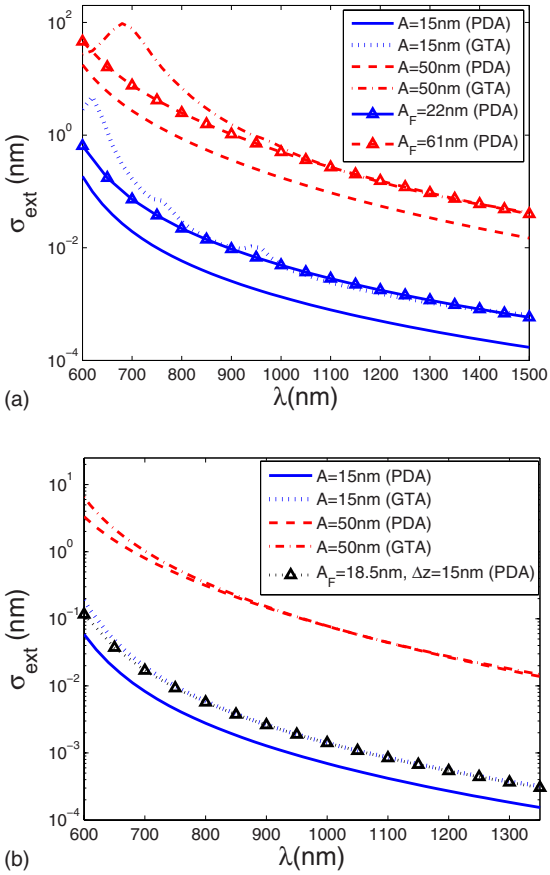

FIG. 6. (Color online) SPP extinction spectrum for gold cubic particles with side dimension A and the particle-to-surface gap Δz (Fig. 1) calculated using both the Green's tensor approach (GTA) and the point-dipole approximation (PDA). (a) $\Delta z=0$; $A_F=22$ nm and $A_F=61$ nm are the fitting sizes, which determine the fitting radius $R_p=[(3/4\pi)^{1/3}A_F]$ in the PDA calculations, for cubes $A=15$ nm and $A=50$ nm, respectively. (b) $\Delta z=A$; $A_F=18.5$ nm is the fitting size for the fitting radius $R_p=[(3/4\pi)^{1/3}A_F]$ in the PDA calculation for the cube of $A=15$ nm and $\Delta z=15$ nm.

rapidly on increasing the size of the scatterer. As a result for relatively large particles, we have a more complex correlation between the PDA and finite-size calculations (Fig. 7). For large scatterers, the PDA extinction cross sections can be larger than the extinction calculated for finite-size scatterers in the region of relatively small wavelengths. As the size of a scatterer increases, the wavelength at which the PDA extinction is equal to the extinction of the finite-size scatterer is shifted toward longer wavelengths [Fig. 7(a)]. When the influence of the metal surface on the extinction is small [Fig. 7(b)], the two approaches give similar results at large wavelengths, where the dipole moment dominates over the rest of the multipole contributions to the total scattering.

Thus, our investigation has shown that the PDA is quite suited for the description of SPP scattering by nanoparticles (cubes) in the case of weak interaction between scatterer and metal surface with SPP and far away from the resonance conditions.

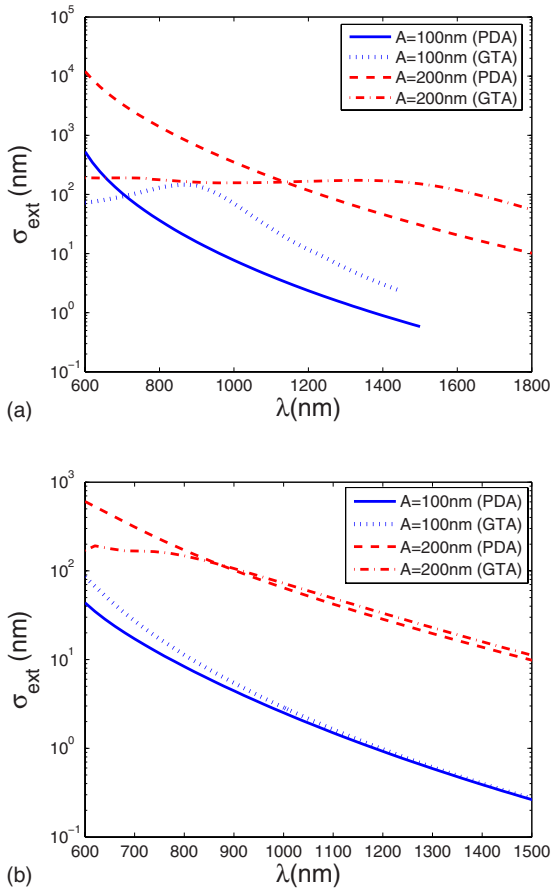

FIG. 7. (Color online) SPP extinction spectrum for gold cubic particles with side dimension A and the particle-to-surface gap Δz (Fig. 1) calculated using both the Green's tensor approach (GTA) and the point-dipole approximation (PDA). (a) $\Delta z=0$; (b) $\Delta z=A$.

V. CONCLUSIONS

In this paper, we have analyzed the SPP scattering by a finite-size nanoparticle placed in the vicinity of a dielectric-metal interface. The Green's function formalism has been employed paying special attention to the determination of scattered fields and differential and total cross sections for different scattering channels, namely, for the elastic SPP-to-SPP scattering and SPP scattering into free-space waves propagating away from the interface. The expressions obtained quantify the influence of both material and configurational parameters on the scattering process. The SPP absorption by a nanoparticle has been considered using the PDA. The general consideration based on the GTA was related to the PDA, focusing on its transition to the PDA in the limit of small particles approximated by spheres of the same volume. The SPP extinction spectra for cubic gold particles of different dimensions placed near a flat gold surface have been calculated so as to study the role of finite-size effects on the SPP scattering. It was found that the extinction spectra feature a resonance corresponding to the LSP mode excited in the cube by the electric field of the incident SPP. The strength and spectral position of the LSP resonance strongly depend on the size of the particle and the particle-to-surface gap. For relatively small particles placed either just on the metal surface or at a small distance from it, comparison between the SPP extinction cross section for cubic particles and that obtained with the PDA showed that the PDA results in significantly smaller scattering cross sections in the considered wavelength range. If the particle-to-surface distance is sufficiently large, the exact calculations and the PDA results were found rather similar in the wavelength range far away from the LPS resonance. Furthermore, it was found that, for nonresonant wavelengths and particles being located close to the surface, one can still apply the PDA and obtain good agreement with the exact calculations if the particle volume is used as a fitting parameter in the PDA. Even for relatively large particles, the PDA was found quite accurate once the particle-to-surface distance was sufficiently large. The comparison performed on the two approaches indicates that SPP modeling based on the PDA should be expected to provide only a qualitative agreement with experimental data. However, this can be improved by using the particle volume as a fitting parameter. Quantitative agreement requires the usage of accurate calculations, for example, based on the GTA, especially for the wavelengths close to the LSP resonance. We believe that the presented results should be useful for further understanding and modeling of various SPP scattering phenomena with nonspherical finite-size particles being used, for example, to realize SPP microcomponents.

ACKNOWLEDGMENTS

The authors would like to thank the European Network of Excellence Plasmo-Nano-Devices (FP6-2002-IST-1-507879) and the STREP "Surface Plasmon Photonics" (FP6-NMP4-CT2003-505699). A.B.E. is grateful to the Russian Foundation for Basic Research, Grant No. 06-02-16443, for the support. Also, A.B.E. expresses his greatest appreciation of the kind hospitality of the entire staff of the Departamento de Fisica de la Materia Condensada, Universidad de Zaragoza where this research was partially carried out.

*a.b.evlyukhin@mail.ru

[1] *Surface Polaritons*, edited by V. M. Agranovich and D. L. Mills (North-Holland, Amsterdam, 1982); H. Raether, *Surface Plasmon*, Springer Tracts in Modern Physics Vol. 111 (Springer, Berlin, 1988).

[2] W. L. Barnes, A. Dereux, and T. W. Ebbesen, Nature (London) **424**, 824 (2003).

[3] A. V. Zayats, I. I. Smolyaninov, and A. A. Maradudin, Phys. Rep. **408**, 131 (2005).

[4] J. C. Weeber, A. Dereux, C. Girard, J. R. Krenn, and J. P. Goudonnet, Phys. Rev. B **60**, 9061 (1999).

[5] P. Berini, Phys. Rev. B **61**, 10484 (2000).

[6] B. Lamprecht, J. R. Krenn, G. Schider, H. Ditbacher, M. Salermo, N. Felidj, A. Leatner, and F. R. Aussenegg, Appl. Phys. Lett. **79**, 51 (2001).
[7] J. C. Weeber, J. R. Krenn, A. Dereux, B. Lamprecht, Y. Lacroute, and J. P. Goudonnet, Phys. Rev. B **64**, 045411 (2001).
[8] J. C. Weeber, Y. Lacroute, and A. Dereux, Phys. Rev. B **68**, 115401 (2003).
[9] J. A. Sánchez-Gil, Appl. Phys. Lett. **73**, 3509 (1998).
[10] J. A. Sánchez-Gil and A. A. Maradudin, Phys. Rev. B **60**, 8359 (1999).
[11] J. C. Weeber, Y. Lacroute, A. Dereux, E. Devaux, T. Ebbesen, C. Girard, M. U. Gonzalez, and A.-L. Baudrion, Phys. Rev. B **70**, 235406 (2004).
[12] F. López-Tejeira, F. J. García-Vidal, and L. Martín-Moreno, Phys. Rev. B **72**, 161405(R) (2005).
[13] J. Gómez Rivas, M. Kuttge, H. Kurz, P. Haring Bolivar, and J. A. Sánchez-Gil, Appl. Phys. Lett. **88**, 082106 (2006).
[14] A. Yu. Nikitin and L. Martín-Moreno, Phys. Rev. B **75**, 081405(R) (2007).
[15] A. Yu. Nikitin, F. López-Tejeira, and L. Martín-Moreno, Phys. Rev. B **75**, 035129 (2007).
[16] F. López-Tejeira, S. G. Rodrigo, L. Martín-Moreno, F. J. García-Vidal, E. Devaux, T. W. Ebbesen, J. R. Krenn, I. P. Radko, S. I. Bozhevolnyi, M. U. Gonzalez, J. C. Weeber, and A. Dereux, Nat. Phys. **3**, 324 (2007).
[17] I. V. Novikov and A. A. Maradudin, Phys. Rev. B **66**, 035403 (2002).
[18] S. I. Bozhevolnyi, V. S. Volkov, E. Devaux, and T. W. Ebbesen, Phys. Rev. Lett. **95**, 046802 (2005).
[19] S. I. Bozhevolnyi, V. S. Volkov, E. Devaux, J. Y. Laluet, and T. W. Ebbesen, Nature (London) **440**, 508 (2006).
[20] E. Moreno, F. J. García-Vidal, S. G. Rodrigo, L. Martín-Moreno, and S. I. Bozhevolnyi, Opt. Lett. **31**, 3447 (2006).
[21] I. I. Smolyaninov, D. L. Mazzoni, J. Mait, and C. C. Davis, Phys. Rev. B **56**, 1601 (1997).
[22] H. Ditlbacher, J. R. Krenn, G. Schider, A. Leitner, and F. R. Aussenegg, Appl. Phys. Lett. **81**, 1762 (2002).
[23] J. R. Krenn, H. Ditlbacher, G. Schider, A. Hohenau, A. Leitner, and F. R. Aussenegg, J. Microsc. **209**, 167 (2003).
[24] A. L. Stepanov, J. R. Krenn, H. Ditlbacher, A. Hohenau, A. Drezet, B. Steinberger, A. Leitner, and F. R. Aussenegg, Opt. Lett. **30**, 1524 (2005).
[25] S. Bozhevolnyi and V. Volkov, Opt. Commun. **198**, 241 (2001).
[26] T. Søndergaard and S. I. Bozhevolnyi, Phys. Rev. B **67**, 165405 (2003).
[27] S. I. Bozhevolnyi, J. Erland, K. Leosson, P. M. W. Skovgaard, and J. M. Hvam, Phys. Rev. Lett. **86**, 3008 (2001).
[28] S. I. Bozhevolnyi, V. S. Volkov, K. Leosson, and A. Boltasseva, Appl. Phys. Lett. **79**, 1076 (2001).
[29] T. Søndergaard and S. I. Bozhevolnyi, Phys. Rev. B **71**, 125429 (2005).
[30] I. P. Radko, T. Søndergaard, and S. I. Bozhevolnyi, Opt. Express **14**, 4107 (2006).
[31] A.-L. Baudrion, J.-C. Weeber, A. Dereux, G. Lecamp, P. Lalanne, and S. I. Bozhevolnyi, Phys. Rev. B **74**, 125406 (2006).
[32] B. T. Draine, Astrophys. J. **333**, 848 (1988).
[33] C. Girard and A. Dereux, Phys. Rev. B **49**, 11344 (1994).
[34] A. B. Evlyukhin and S. I. Bozhevolnyi, Phys. Rev. B **71**, 134304 (2005).
[35] S. I. Bozhevolnyi and V. Coello, Phys. Rev. B **58**, 10899 (1998).
[36] I. P. Radko, S. I. Bozhevolnyi, A. B. Evlyukhin, and A. Boltasseva, Opt. Express **15**, 6576 (2007).
[37] V. Coello, T. Søndergaard, and S. I. Bozhevolnyi, Opt. Commun. **240**, 345 (2004).
[38] A. B. Evlyukhin, S. I. Bozhevolnyi, A. L. Stepanov, and J. R. Krenn, Appl. Phys. B **84**, 29 (2006).
[39] A. B. Evlyukhin and S. I. Bozhevolnyi, JETP Lett. **81**, 218 (2005).
[40] K. L. Kelly, E. Coronado, L. L. Zhao, and G. C. Schatz, J. Phys. Chem. B **107**, 668 (2003).
[41] J. P. Kottmann, O. J. F. Martin, D. R. Smith, and S. Schultz, Phys. Rev. B **64**, 235402 (2001).
[42] U. Hohenester and J. Krenn, Phys. Rev. B **72**, 195429 (2005).
[43] A. Hohenau, J. R. Krenn, G. Schider, H. Ditlbacher, A. Leitner, F. R. Aussenegg, and W. L. Schaich, Europhys. Lett. **69**, 538 (2005).
[44] A. B. Evlyukhin and S. I. Bozhevolnyi, Surf. Sci. **590**, 173 (2005).
[45] M. I. Tribelsky and B. S. Luk'yanchuk, Phys. Rev. Lett. **97**, 263902 (2006).
[46] Z. B. Wang, B. S. Luk'yanchuk, M. H. Hong, Y. Lin, and T. C. Chong, Phys. Rev. B **70**, 035418 (2004).
[47] A. V. Shchegrov, I. V. Novikov, and A. A. Maradudin, Phys. Rev. Lett. **78**, 4269 (1997).
[48] Chen-To Tai, *Dyadic Green's Functions in Electromagnetic Theory* (IEEE, New York, 1994).
[49] O. J. F. Martin, C. Girard, and A. Dereux, Phys. Rev. Lett. **74**, 526 (1995).
[50] L. Novotny, J. Opt. Soc. Am. A **14**, 105 (1997).
[51] M. Paulus and O. J. F. Martin, J. Opt. Soc. Am. A **18**, 854 (2001).
[52] T. Søndergaard and S. I. Bozhevolnyi, Phys. Rev. B **69**, 045422 (2004).
[53] E. Palik, *Handbook of Optical Constant of Solids* (Academic, San Diego, CA, 1985).
[54] C. Girard and A. Dereux, Rep. Prog. Phys. **59**, 657 (1996).
[55] M. Born and E. Wolf, *Principles of Optics* (Pergamon, Oxford, 1970).
[56] L. D. Landau and E. M. Lifshitz, *Electrodynamics of Continuous Media*, Course of Theoretical Physics Vol. 8 (Pergamon, New York, 1984).
[57] A. B. Evlyukhin, Tech. Phys. Lett. **31**, 817 (2005).
[58] O. Keller, M. Xiao, and S. Bozhevolnyi, Surf. Sci. **280**, 217 (1993).
[59] G. Lévêque and O. J. F. Martin, Opt. Lett. **31**, 2750 (2006).
[60] G. Lévêque and O. J. F. Martin, Opt. Express **14**, 9971 (2006).
[61] L. Novotny, B. Hecht, and D. W. Pohl, J. Appl. Phys. **81**, 1708 (1997).
[62] R. Fuchs, Phys. Rev. B **11**, 1732 (1975).
[63] C. Noguez, J. Phys. Chem. C. **111**, 3806 (2007).
[64] C. F. Bohren and D. R. Huffman, *Absorption and Scattering of Light by Small Particles* (Wiley, New York, 1983).